

## Piezoconductivity of graphene nanoribbons. Elastic-plastic deformations

© O.S. Lebedeva, N.G. Lebedev

Volgograd State University,  
Volgograd, Russia,

E-mail: nikolay.lebedev@volsu.ru

Received December 24, 2023

Revised March 5, 2024

Accepted March 5, 2024

In this work, the piezo resistive properties of a two-dimensional material are studied using the example of a fragment of graphene nanoribbons of the „arm-chair“ and „zig-zag“ types. The dependence of the longitudinal component of the piezoconductivity tensor of nanoribbons on the value of a relative elastic-plastic deformation is analyzed. It has been shown that conductive ribbons exhibit stable piezo resistive properties which do not depend on its width, but depend only on the structural modification of the zig-zag or arm-chair. Small plastic deformations abruptly change the longitudinal component for zig-zag ribbons by an order of magnitude more than for arm-chair ribbons. Semiconductor ribbons of relatively small width have a „hyperpiezo resistance“ effect, which disappears with increasing the ribbon width in proportion to the decrease in the band gap.

**Keywords:** straintronics, graphene, nanoribbons, piezo resistive effect, elastic-plastic deformations.

DOI: 10.61011/PSS.2024.04.58205.254

### 1. Introduction

Straintronics as one of the branches of the scientific discipline of condensed matter physics formed at the beginning of the 21st century [1] is aimed at studying the effect of mechanical stresses on the electronic properties of a substance. A change of the energy gap and conductivity of deformed semiconductors and dielectrics results in a piezoelectric effect. The piezo resistive effect is based on the sensitivity of the electrical resistance (or electrical conductivity) of materials in relation to mechanical load. It is based on the basic principles of operation of electromechanical energy conversion devices, such as sensors, piezo resistors, pressure sensors, etc. The discovery of this effect has become an important prerequisite for the emergence and development of MEMS (MicroElectroMechanicalSystem) technologies used for the integration of mechanical elements and sensors on a silicon substrate.

The history of the discovery of the piezo resistance effect, or piezo resistive effect, is associated with the name of Dr. Charles S. Smith [2]. His work presents the results of studies of the effect of uniaxial deformations on electrical resistance in semiconductors. Smith found that the change of the resistance of germanium and silicon *p*- and *n*-types when a mechanical load is applied to them can be ten times greater than for materials with metallic conductivity (for example, metals). The results of experimental data on the determination of the piezo resistance tensor (one of the main characteristics of the piezo resistive effect) are presented in the article. Smith's discovery served as an impetus for the emergence of new areas of practical application of semiconductors, for example, such as tensometry, which studies the basics of creating semiconductor strain gages and load cells [3,4].

The piezo resistive effect can be characterized by the coefficients of elastoplasticity, elastoresistance, or the so-called calibration factor [5]. The experimental data allow determining the coefficients of piezo resistance or elastoresistance and the calibration factor, and the coefficients of elastoplasticity can be calculated using theoretical methods.

The study of deformation effects in low-dimensional structures, for example, the graphene family, creates the necessary conditions for the development of „flexible electronics“ [6]. One of the attractive properties of such materials is the ability to significant elastic deformation. Graphene [7,8] contains a unique combination of properties that is found nowhere else: conductivity and transparency, mechanical strength and elasticity. It can successfully replace many materials in a huge number of electronics, spintronics and sensors devices. At the same time, the main advantage of graphene complicates its use it as a basis for the development of components of modern electronics because of almost complete absence of a band gap ( $E_g < 0.05$  MeV), which makes it impossible to close the channel of a field-effect transistor based on it. This makes it difficult to use it as a basis for electromechanical energy conversion devices such as transistors, resistors, piezo resistive sensors, pressure transmitters.

Graphene at present stage is classified as isotropic linear elastic materials that obey Hooke's law at low deformations. The deviations from linearity are observed in case of large deformations, and the fluidity property begins to manifest itself, which is modeled by adding a quadratic term in deformation to the linear Hooke law [6]. Small plastic deformations in graphene can be caused by dislocations of various types [9], as well as defects of the „Stone–Wales“ type, which can be considered as dislocation dipoles [10].

The impact of the size of loop dislocations on the electronic properties and sublattice ferrimagnetism in graphene was studied in [11], using the density functional theory methods. The authors modeled the interface of the Co(0001) surface and a gold monolayer with triangular loop dislocations, on which a graphene layer was placed. It is shown in this paper that graphene and the underlying gold layer with loop dislocations of various sizes are characterized by ferrimagnetic ordering within atomic layers. Moreover, the presence of additional gold adatoms under graphene enhances the induced spin-orbit interaction in graphene and opens an energy gap, but does not destroy the ferrimagnetic order in graphene. The control of the number and size of clusters as a result of intercalation can be used to enhance the induced Rashba interaction and obtain a stable topological phase in graphene.

The results of a study of the piezoconductive properties of two-dimensional graphene family structures such as graphene nanoribbons (GNRs) of armchair and zigzag types taking into account small plastic deformations are presented in this paper.

## 2. A model of the electronic structure of deformed graphene

The geometric model of nanoribbons (NR) is chosen based on a two-dimensional hexagonal layer with two atoms in a lattice cell (LC) and vectors of the main translations of  $\mathbf{a}_1 = a(1, 0)$  and  $\mathbf{a}_2 = a(-1/2, \sqrt{3}/2)$  ( $a_1 = a_2 = a$ ),  $a = \sqrt{3}R_0$  — the lattice constant,  $R_0 = 1.42 \text{ \AA}$  — the interatomic distance in graphene (Figure 1).

The corresponding graphene nanoribbons (GNR) will be obtained if an incision is made on the graphene plane along the armchair or zigzag direction. GNRs are classified using a single index  $N$  [7]. Traditionally, zigzag nanoribbons are denoted by  $N$ -ZGNR, where  $N$  is equal to the number of carbon atoms that fit in the cross section of the ribbon,

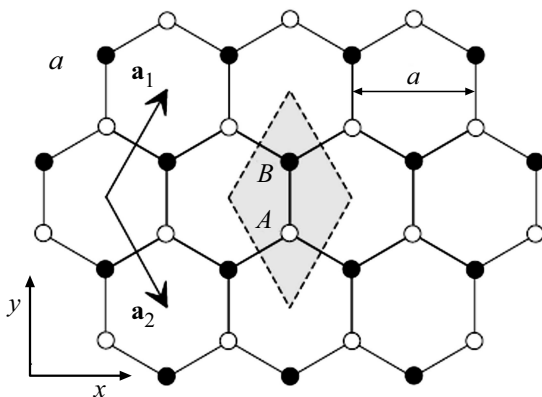


**Figure 1.** An elementary cell of a hexagonal crystal lattice of graphene with two atoms in an elementary cell and vectors of basic translations  $\mathbf{a}_1 = a(1, 0)$  and  $\mathbf{a}_2 = a(-1/2, \sqrt{3}/2)$  ( $a_1 = a_2 = a$ ),  $a$  is a lattice constant [12].

and  $N$ -AGNR are armchair ribbons, for which the index  $N$  is equal to the number of carbon dimers on the slice. The GNR width is also expressed in terms of the index  $N$  using the following formula [7]:

$$H = \begin{cases} \left(\frac{3}{2}N - 1\right)R_0 \equiv H_z, \\ \frac{\sqrt{3}}{2}(N - 1)R_0 \equiv H_a, \end{cases} \quad (1)$$

where  $H_z$  — the width of the zigzag ribbon,  $H_a$  — the width of the armchair ribbon.

The main features of the band structure of the GNR are described within the framework of the strong coupling approximation for the  $\pi$ -electronic system. The electronic spectrum of graphene  $\varepsilon(k_x, k_y)$  is considered as a starting point [12]:

$$\varepsilon(k_x, k_y) = \pm \gamma \left\{ 1 + 4 \cos\left(\frac{3k_x R_0}{2}\right) \cos\left(\frac{\sqrt{3}k_y R_0}{2}\right) + 4 \cos^2\left(\frac{\sqrt{3}k_y R_0}{2}\right) \right\}^{1/2}, \quad (2)$$

where  $\mathbf{k} = (k_x, k_y)$  — the electron wave vector in the Brillouin zone,  $\gamma = 2.7 \text{ eV}$  — the integral of transition (matrix element of the transition) of an electron from one node to another. The electronic spectrum of nanoribbons is defined as the lines of intersection of the two-dimensional energy surface of graphene with parallel planes of the allowed values of the wave vector  $q = 2\pi n/H$  ( $n = 1, 2, \dots$ ) directed across the ribbon.

Then the condition for quantization of the wave vector  $\mathbf{k}$  in the transverse direction, taking into account the closure of the boundary carbon atoms by hydrogen atoms, is determined from the condition that the wave function at the boundary of the ribbon, namely, on atomic series numbered 0 and  $N + 1$ , is equal to zero [13]. As a result, the electronic spectrum of graphene NR of armchair and zigzag types can be represented in the following form

$$\varepsilon_a(k, n) = \pm \gamma \sqrt{1 + 4 \cos\left(\frac{ka_x}{2}\right) \cos\left(\frac{\pi n}{N+1}\right) + 4 \cos^2\left(\frac{\pi n}{N+1}\right)}, \quad (3)$$

$$\varepsilon_z(k, n) = \pm \gamma \sqrt{1 + 4 \cos\left(\frac{\pi n}{N}\right) \cos\left(\frac{ka_y}{2}\right) + 4 \cos^2\left(\frac{ka_y}{2}\right)}, \quad (4)$$

$$n = 1, 2, \dots, N,$$

where  $k$  — the longitudinal component of the wave vector,  $a_x = 3R_0$  — the lattice constant of armchair ribbons,  $a_y = \sqrt{3}R_0$  — the lattice constant of zigzag ribbons.

All zigzag nanoribbons are conductors within the framework of the considered electronic structure model, as well as armchair nanoribbons with the index  $N = 3m - 1$ , where  $m$  is an integer. Accordingly, the armchair nanoribbons with indices  $N = 3m$  and  $N = 3m + 1$  exhibit semiconductor properties, i.e. they have a small gap in the spectrum at the Fermi level, which decreases with an increase of the ribbon width [7]:

$$E_g = \begin{cases} 0, & N = 3m - 1, \\ \frac{\pi R_0}{H_a + \frac{\sqrt{3}}{2} R_0}, & N = 3m, \\ \frac{\pi R_0}{H_a}, & N = 3m + 1. \end{cases} \quad (5)$$

The deformed state of the crystallite is generally characterized by the distortion tensor  $u_{\alpha\beta} = \partial_\beta(\mathbf{r}' - \mathbf{r})_\alpha$ , ( $\alpha, \beta = x, y, z$ ), where  $\mathbf{r}$  and  $\mathbf{r}'$  — the radius vectors of the initial and final positions of some point of the crystallite [14]. The diagonal elements of the tensor characterize the relative elongation of the sample along the corresponding direction, the non-diagonal elements set the angle of rotation of the linear element in case of deformation.

The deformation of longitudinal tension (compression) changes the shape of the lattice cell and the Brillouin zone (BZ). The length of the LC increases (decreases) in case of tension (compression), and the length of the BZ decreases (increases) accordingly. Transformations of the LC and BZ of low-dimensional structures, such as carbon nanotubes and graphene nanoribbons, were described in detail in [15–19]. We will provide only a brief description here. Let's denote the magnitude of the relative deformation of GNR by  $\delta = \Delta a/a_0$ , where  $\Delta a = a - a_0$  — the change of the lattice constant of a one-dimensional crystallite,  $a_0$  — the equilibrium lattice constant of GNR. Then the current value of the deformed lattice constant is  $a = a_0(1 + \delta)$ .

The change of the width of the ribbon as a result of tension (compression) deformation can be taken into account using the Poisson's ratio  $\nu$ , which has the values 0.15–0.45 for GNR [6]:

$$H = H_0(1 - \nu\delta), \quad (6)$$

where  $H_0$  — the width of the undeformed GNR.

Deformation of the elements of a body under stress under the action of a system of forces generally consists of reversible  $\delta$ , or elastic, and residual  $\delta_p$ , or plastic parts [20]. That is, the change of the lattice constant of the crystallite is attributable to the elastic and plastic deformation  $a = a_0(1 + \delta + \delta_p)$  [14].

Therefore, taking into account the above, it is possible to propose a phenomenological electronic spectrum of deformed chair-type and zigzag-type GNRs in the following

form:

$$\begin{aligned} \varepsilon_a(k, n) = & \pm\gamma(\delta + \delta_p) \left\{ 1 + 4 \cos\left(\frac{\pi n}{N+1}\right) \right. \\ & \times \cos\left[\frac{3}{2}kR_0(1 + \delta + \delta_p)\right] + 4 \cos^2\left(\frac{\pi n}{N+1}\right) \left. \right\}^{1/2}, \\ -\pi < & 3kR_0(1 + \delta + \delta_p) \leq \pi, \quad n = 1, \dots, N, \quad (7) \end{aligned}$$

$$\begin{aligned} \varepsilon_z(k, n) = & \pm\gamma(\delta + \delta_p) \left\{ 1 + 4 \cos\left[\frac{\sqrt{3}}{2}kR_0(1 + \delta + \delta_p)\right] \right. \\ & \times \cos\left(\frac{\pi n}{N}\right) + 4 \cos^2\left[\frac{\sqrt{3}}{2}kR_0(1 + \delta + \delta_p)\right] \left. \right\}^{1/2}, \\ -\pi < & \sqrt{3}kR_0(1 + \delta + \delta_p) \leq \pi, \quad n = 1, \dots, N. \quad (8) \end{aligned}$$

The dependence of the hopping integral  $\gamma(\delta)$  on relative deformation was calculated within the framework of density functional theory using the exchange-correlation potential B3LYP in the basis of atomic orbitals STO-3G. A graphene surface fragment with a size of  $6 \times 6$  lattice cells was considered to perform quantum chemical calculations. The boundary unsaturated bonds were closed by monovalent hydrogen atoms. The deformation of the structure along the „arm-chair“ and „zig-zag“ directions was modelled by stepwise freezing of atoms at opposite boundaries of the fragment. The obtained numerical values of the dependence  $\gamma(\delta)$  were interpolated using the following analytical expression:

$$\gamma = \gamma_0 \exp(-2.0162R), \quad R = R_0(1 + \delta), \quad \gamma_0 = 47.42 \text{ eV}. \quad (9)$$

The changes of the band structure of conductive and semiconductor GNR in the presence of small plastic deformations are shown in Figure 2.

The values of relative tensile (compression) deformation  $\delta = \pm 0.1, \pm 0.06, \pm 0.04, \pm 0.02, \pm 0.01$  were used in the calculations. The plastic deformation was accounted for by the addition of  $\delta_p = 0.015$ .

### 3. Piezoconductivity of graphene nanoribbons

The definition of the piezoconductivity tensor of two-dimensional crystal structures of the graphene family can be written as follows according to [5]

$$\frac{\sigma_{\alpha\beta}}{\langle\sigma\rangle} = M_{\alpha\beta\chi\eta} \cdot \delta_{\chi\eta}, \quad \langle\sigma\rangle = \frac{1}{2} \text{Sp}[\sigma] = \frac{\sigma_{xx} + \sigma_{yy}}{2}, \quad (10)$$

where  $\sigma_{\alpha\beta}$  — the specific conductivity tensor,  $\delta_{\chi\eta}$  — the strain tensor,  $M_{\alpha\beta\chi\eta}$  — the piezo conductivity tensor of the 4th order,  $\alpha, \beta, \chi, \eta = x, y$ .

A so-called piezoresistive constant can be introduced for two-dimensional structures as a diagonal element  $M = M_{xxxx}$  or  $M_{yyyy}$  in the case of uniaxial stretching along armchair or zigzag directions, respectively.

The longitudinal component can be found using the following expression for the case of quasi-one-dimensional structures such as GNR:

$$M = \frac{\Delta\sigma}{\sigma_0} \frac{1}{\delta}, \quad (11)$$

where  $\Delta\sigma = \sigma - \sigma_0$  — the change in the longitudinal component of the specific conductivity tensor due to deformation;  $\sigma_0$  — the longitudinal component  $\sigma_{xx}$  (for armchair nanoribbons) or  $\sigma_{yy}$  (for zigzag nanoribbon) of the 2nd rank specific conductivity tensor of undeformed nanoribbons,  $\sigma$  — the same component  $\sigma_{xx}$  or  $\sigma_{yy}$  deformed nanoribbons.

Accordingly, the calibration factor  $K$  [5], which determines the relative change of the resistance of a one-dimensional material, is expressed using the following formula:

$$K = \frac{\Delta P}{P} \frac{1}{\delta} \quad \text{or} \quad P = P(1 + K\delta), \quad (12)$$

where  $P_0$  — the resistance of the undeformed sample,  $P$  — the resistance of the deformed sample. The coefficient can be measured experimentally, and the formula (12) is used to calibrate piezoresistors, load cells, etc.

The relationship between the values  $K$  and  $M$  can be expressed by the following ratio

$$K = \left( \frac{-M\delta}{M\delta + 1} \right) \frac{1}{\delta} = \frac{-M}{M\delta + 1}.$$

The sum  $\delta + \delta_p$  should be used for the case of elastic-plastic deformations in formulas (11) and (12), instead of elastic relative deformation  $\delta$ .

The expression for calculating the longitudinal component  $\sigma$  of the specific conductivity tensor GNR, obtained within the framework of Kubo–Greenwood theory using the function method and the strong coupling model Hamiltonian, presented in [18]:

$$\sigma = \frac{e^2}{k_B T V} \times \sum_{\mathbf{k}, \beta} \sum_{\mathbf{q}, \lambda} v(\mathbf{k}) v(\mathbf{q}) \langle n_{\mathbf{k}\beta} \rangle \left[ \langle n_{\mathbf{q}\lambda} \rangle + \delta_{\mathbf{kq}} \delta_{\beta\lambda} \left( 1 - \langle n_{\mathbf{k}\beta} \rangle \right) \right], \quad (13)$$

where  $V = H \cdot L \cdot d$  — the volume of the nanoribbon,  $H$  — the width and  $L$  — the length of the GNR,  $d$  — the covalent diameter of the carbon atom;  $T$  — the absolute temperature;  $e$  — the elementary charge;  $\mathbf{k}$ ,  $\mathbf{q}$  — two-component wave vectors within the Brillouin zone;  $\beta$ ,  $\lambda$  — the spin indices;  $v(\mathbf{k})$  — the longitudinal component of the electron velocity vector in the zone ZB;  $\langle n_{\mathbf{k}\beta} \rangle$  — the average number of particles in a quantum state with a wave vector  $\mathbf{k}$  and spin  $\beta$ , expressed by the Fermi–Dirac distribution function:

$$\langle n_{\mathbf{k}\beta} \rangle = \left[ 1 + \exp \left( \frac{\varepsilon_{\beta}(\mathbf{k}) - \mu}{k_B T} \right) \right]^{-1},$$

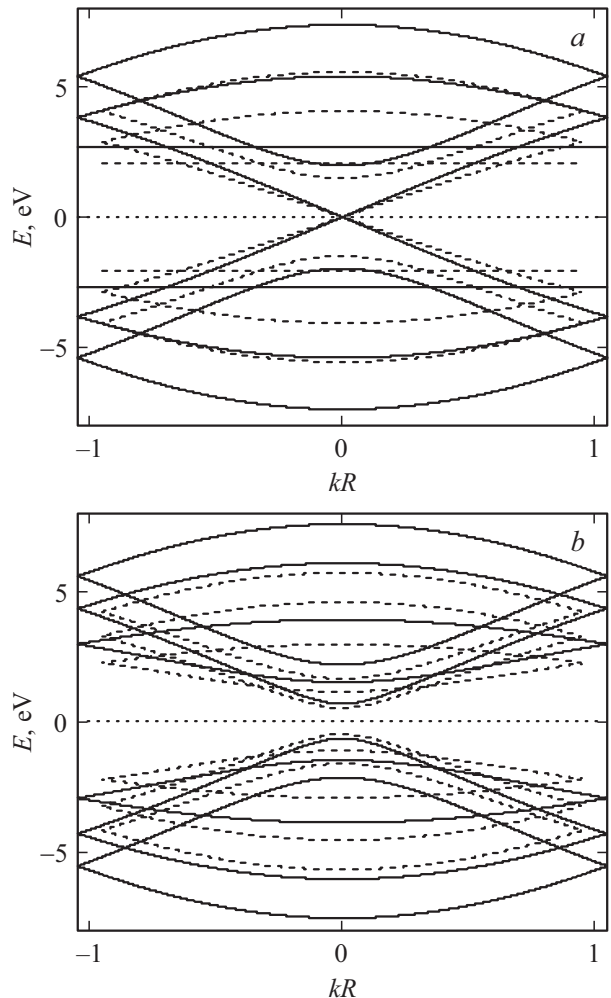


**Figure 2.** The zone structure of undeformed (solid line) and deformed (dotted line) graphene nanoribbons 5-AGNR (a) and 6-AGNR (b) at  $\delta = 0.1$ . The energy is counted from the Fermi level.

where  $\varepsilon_{\beta}(\mathbf{k})$  — the energy of the electron state with a wave vector  $\mathbf{k}$  and spin  $\beta$ ,  $k_B$  — the Boltzmann constant;  $\mu$  — the chemical potential, which is found using the self-consistency procedure from the condition of normalization of the distribution function to the full number of  $\pi$ -electrons  $N_e$  in the system

$$N_e = \sum_{\mathbf{k}, \beta} \langle n_{\mathbf{k}\beta} \rangle.$$

The number of  $\pi$ -electrons is determined by the number of atoms in the crystallite, taking into account the half-filling of the zone. The number of electrons increases (decreases) by the number of defects  $N_d$  in the presence of donor (acceptor) defects.

The velocity vector  $\mathbf{v}(\mathbf{k})$  is determined in a standard way through the energy of electrons in the Brillouin zone (7) and (8):

$$\mathbf{v}(\mathbf{k}) = \frac{1}{\hbar} \frac{\partial \varepsilon(\mathbf{k})}{\partial \mathbf{k}}.$$

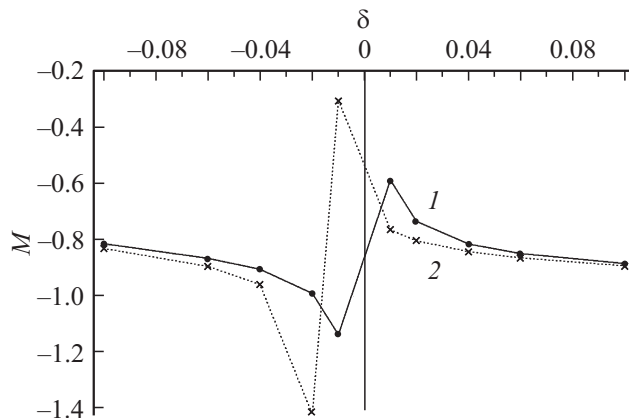
#### 4. Discussion

The results of the study of the piezoresistive properties of armchair and zigzag-shaped GNRs of different widths and with different types of conductivity, designated as  $N$ -AGNR and  $N$ -ZGNR, respectively, are presented in this paper.

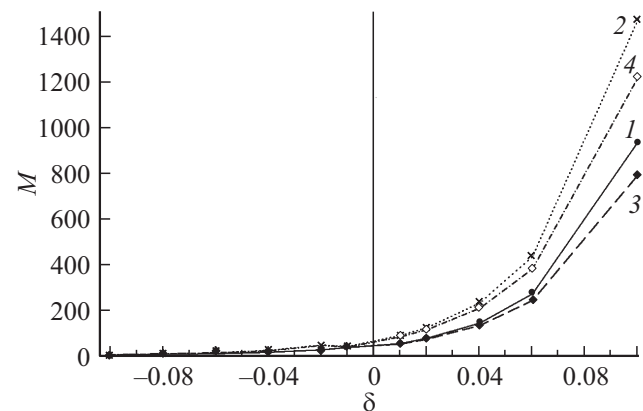
Figures 3–5 shows the calculated functional dependences of the longitudinal component of the piezoconductivity tensor  $M(\delta)$  on tensile and compression deformations  $\delta$  of conductive and semiconductor nanoribbons. The lines on the graphs connect the calculated points to identify the nature of the change in the function  $M(\delta)$ . The calculations were performed at a temperature of  $T = 300$  K. The minimum nanoribbon length of  $L = 10^6 a$  was set in calculations. The calculation results did not change with a further increase of the length of the GNR.

Figure 3 clearly demonstrates that the component  $M$  takes negative values over the entire range of magnitude  $\delta$  in the case of conductive chair-type nanoribbons 8-AGNR. A monotonous decrease of the function  $M(\delta)$  is observed with compression ( $\delta < 0$ ) and tensile ( $\delta > 0$ ) deformations. Its behavior is fully explained by the changes of the nanoribbon band structure caused by deformation. A negative value of  $M$  in the compression region means that the specific conductivity increases. In addition, the function  $M(\delta)$  increases in the direction of compression. This effect is a consequence of the competition of several processes: an increase of the hopping integral and a decrease of the density of states near the Fermi level because of an increase of the width of the conduction band and the slope of the dispersion lines in the vicinity of the Dirac point (Figure 2).

The increase of  $\delta$  in the tensile range reduces the hopping integral, the width of the conduction band, and the slope of the dispersion lines near the point  $K$  and increases the density of states in the near-Fermi region. But at the



**Figure 3.** Dependence of the longitudinal component  $M(\delta)$  of conductive graphene nanoribbons of 8-AGNR, 50-AGNR, 8-ZGNR, 9-ZGNR, 10-ZGNR and 50-ZGNR type on the magnitude of relative deformation  $\delta$  in case of elastic tensile-compression deformations (1) and elastoplastic deformations with  $\delta_p = 0.015$  (2).



**Figure 4.** Dependence of the longitudinal component  $M(\delta)$  of semiconductor graphene nanoribbons 9-AGNR and 10-AGNR on the magnitude of relative deformation  $\delta$ : 9-AGNR, elastic strain of tension-compression (1), 9-AGNR, elastoplastic deformations with  $\delta_{pl} = 0.015$  (2), 10-AGNR, elastic tensile-compression deformations (3), 10-AGNR, elastoplastic deformations with  $\delta_{pl} = 0.015$  (4).

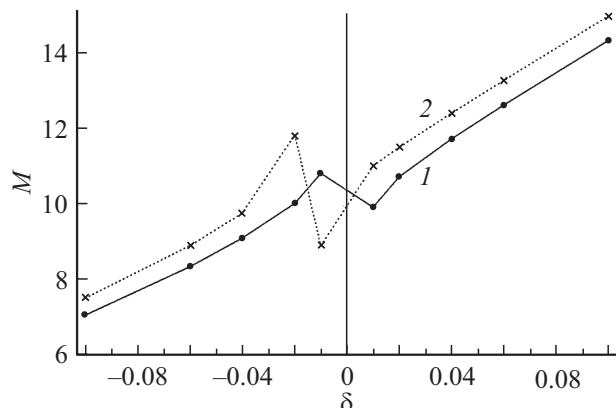


**Figure 5.** Dependence of the longitudinal component  $M(\delta)$  of conductive graphene nanoribbons of 51-AGNR, 52-AGNR type (the dependencies are almost the same) on the magnitude of the relative deformation  $\delta$  with elastic tensile-compression deformations (1) and elastoplastic deformations with  $\delta_p = 0.015$  (2).

same time, the energy of the electrons and their velocity in the Brillouin zone decrease. And the specific conductivity of GNR and the piezoresistive characteristic of  $M$  decreases as a result.

The addition of a small plastic deformation  $\delta_{pl} = 0.015$  does not change the main trend of the behavior of the function  $M(\delta)$  (Figure 3). Differences between the two curves are observed in the vicinity of  $\delta_{pl}$ , the curves shift relative to the point  $\delta = 0$ . Therefore, a sharp jump of  $M$  component is observed even in the compression area. These results indicate a high sensitivity of low-width conductive GNR to plastic deformations.

The described behavior of the specific conductivity of GNR as a result of tensile (compression) deformation

is qualitatively consistent with the literature data presented in the review [6].

The piezoresistivity of semiconductor nanoribbons of structural modification of the „arm-chair“ small-width 9-AGNR and 10-AGNR types is demonstrated in Figure 4. The values of the longitudinal component of the elastoconductivity tensor  $M$  are positive over the entire range  $\delta$ . In general, the figure shows a monotonous growth of the function  $M(\delta)$ . The positive value of  $M$  in the area of compression deformations ( $\delta < 0$ ) means that the conductivity of the nanoribbons decreases with deformation. The width of the conduction band and the magnitude of the band gap increase in semiconductor GNRs in case of compression  $E_g$ . These effects result in a decrease of the specific conductivity and, accordingly, the function  $M(\delta)$ .

The value of  $M$  is also positive in the region of expansion deformations ( $\delta > 0$ ) and increases strongly towards the point  $\delta = 0.1$ . The so-called „hyperresistivity“ is observed when the values of  $M$  increase by several orders of magnitude with small deformations.

It should be noted that the graph of the function  $M(\delta)$  for the semiconductor GNR of 10-AGNR type for each fixed deformation  $\delta$  lies lower than for 9-AGNR. This is attributable to the fact that all nanoribbons of the  $3m + 1$  type have a smaller band gap than those of the GNR of  $3m$  type, according to the formula (5). For this reason more charge carriers enter the conduction band as a result of thermal fluctuations due to the Fermi–Dirac distribution.

Plastic deformation  $\delta_{pl}$  does not change the main tendency of the function behavior  $M(\delta)$ , as well as in the case of conductive GNR. A slight change of the behavior of the magnitude of  $M$  is observed in the vicinity of the point  $\delta_{pl}$  because of the „hyperresistivity“ of small width GNR. The curves do not differ quantitatively in the compression deformation region, and the differences of the graphs  $M(\delta)$  become significant in the tensile region. This is a consequence of the effects of reduction of the width of the conduction band and the band gap.

An increase of the width of the conductive armchair ribbon does not affect the behavior of the value  $M$  (Figure 3). Qualitatively and quantitatively, the dependencies  $M(\delta)$  are similar for all conductors. A similar effect was observed for another one-dimensional carbon structures — nanotubes, and is described in detail in Ref. [15–17].

The piezoresistive properties of semiconductor armchair GNR depend on their width, as can be seen in the example of the ribbon 51-AGNR (Figure 5). The effect of „hyperpiezoresistivity“ disappears as can be clearly seen from the figure. The change of the magnitude of  $M$  in the considered range of relative deformation  $\delta$  occurs within 10. The very tendency of the behavior of  $M(\delta)$  remains qualitatively the same as for narrow nanoribbons. Moreover, the changes of the longitudinal component  $M$  are more noticeable, and amount to several units in the vicinity of the point  $\delta_p = 0.015$ . Thus, the presence of small elastoplastic deformations contributes to a change of the specific conductivity for wide semiconductor GNRs.

Such an effect is attributable, in our opinion, to the inversely proportional dependence of the magnitude of the band gap  $E_g$  on the width of the ribbon. The same effect erases the quantitative differences between  $M(\delta)$  of wide ribbons of  $3m + 1$  and  $3m$  type, due to the small band gap.

All zigzag ribbons are conductors according to the electronic structure of GNR within the framework of the strong coupling method, described, for example, in [7], therefore the behavior of the function  $M(\delta)$  (Figure 3) is similar to the behavior of conductive armchair ribbons (Figure 3) and it does not depend on the width of the ribbon. The differences are only in the quantitative value of the longitudinal component  $M$  within the limits of calculation accuracy.

## 5. Conclusion

The work shows that the presence of small plastic deformations in the structure of graphene nanoribbons affects their piezoresistive properties. The qualitative and quantitative behavior of the longitudinal component of the elastoconductivity tensor  $M$  of conductive GNRs of both armchair and zigzag type, does not depend on the width of the ribbon, due to the peculiarities of the band structure of the conductors. Thus, conductive ribbons exhibit stable piezoresistive properties.

Quantitatively, the dependence  $M(\delta)$  of armchair ribbons is higher than this dependence of zigzag ribbons. That is, the specific conductivity changes more strongly during deformation in ZGNR-type nanoribbons. In addition, a small plastic deformation results in the hop in the components  $M$  in zigzag-shaped GNR by an order of magnitude greater than the hop in armchair GNR.

The piezoresistive properties of semiconductor armchair GNR depend on their width, showing the effect of „hyperpiezoresistivity“ for narrow ribbons. The dependence of the properties on the width decreases with the increase of the width in proportion to how the band gap decreases. Therefore, the wide armchair GNR can, as well as conductive ones, exhibit stable piezoresistive properties.

The presented results can be useful for the development and calibration of electronic elements that use the piezoelectric resistance effect, such as transistors (the model [21] was recently proposed), piezoresistors [22], piezosensors, pressure sensors, optical gates and others.

## Funding

The study was supported by grant No. 22-22-20048 (<https://rscf.ru/project/22-22-20048/>) from the Russian Science Foundation and by budgetary funds of the Volgograd Oblast.

## Conflict of interest

The authors declare that there are no conflicts of interest.

## References

- [1] A.A. Bukharaev, A.K. Zvezdin, A.P. Pyatakov, Yu.K. Fetisov. UFN **188**, 12, 1288 (2018). (in Russian).
- [2] C.S. Smith. Phys. Rev. **94**, 6, 42 (1954).
- [3] M. Din. Poluprovodnikovye tenzodatchiki. Energiya, M. (1968) 215 p.
- [4] L.S. Ilyinskaya, A.N. Podmarkov. Poluprovodnikovye tenzodatchiki. Energiya, M. (1966) 118 p. (in Russian).
- [5] G.L. Bir, G.E. Pikus. Simmetriya i deformacionnye effekty v poluprovodnikakh. Nauka, M. (1972). 584 p. (in Russian).
- [6] I.V. Antonova. UFN **192**, 6, 609 (2022). (in Russian).
- [7] P.B. Sorokin, L.A. Chernozatonsky. UFN **183**, 2, 113 (2013). (in Russian).
- [8] L.A. Chernozatonsky, P.B. Sorokin, A.A. Artyukh. Uspekhi khimii **83**, 3, 251 (2014).
- [9] A.L. Kolesnikova, A.E. Romanov. FTT **45**, 9, 1626 (2003). (in Russian).
- [10] A.H. Akhunova, Yu.A. Baimova. FTT **93**, 4, 445 (2023). (in Russian).
- [11] A.G. Rybkin, A.V. Tarasov, A.A. Gogina, A.V. Verezhenkov, A.A. Rybkina. Pisma v ZhETF **117**, 8, 626 (2023). (in Russian).
- [12] Physics of graphene. Series Nanoscience and Technology / Ed. H. Aoki, M.S. Dresselhaus. Springer International Publishing, Switzerland (2014). 345 p.
- [13] K. Wakabayashi, K. Sasaki, T. Nakanishi, T. Enoki. Sci. Technol. Adv. Mater. **11**, 054504 (2010).
- [14] L.D. Landau, E.M. Lifshitz. Teoreticheskaya fizika. Fizmatlit, M. (2003). T. VII. 264 p.
- [15] O.S. Lyapko, N.G. Lebedev. FTT **54**, 7, 1412 (2012). (in Russian).
- [16] O.S. Lebedeva, N.G. Lebedev. Him. Fizika **33**, 10, 73 (2014). (in Russian).
- [17] O.S. Lebedeva, N.G. Lebedev, I.A. Lyapko. Math. Physics and Comp. Simulation **21**, 1, 53 (2018).
- [18] O.S. Lebedeva, N.G. Lebedev, I.A. Lyapko. J. Phys.: Condens. Matter **32**, 14, 145301 (2020).
- [19] O.S. Lebedeva, N.G. Lebedev, I.A. Lyapko. Zhurn. fiz. khimii **94**, 8, 1232 (2020). (in Russian).
- [20] A. Nadai. Plastichnost i razrushenie tverdykh tel. IL, M. (1954). T. 1. 648 p. (in Russian).
- [21] A.C. McRae, G. Wei, A.R. Champagne. Phys. Rev. Appl. **11**, 054019 (2019).
- [22] A. Sinha, A. Sharma, P. Priyadarshi, A. Tulapurkar, B. Muralidharan. Phys. Rev. Res. **2**, 043041 (2020).

*Translated by A.Akhtyamov*